A soluble 3-hydroxy-3-methylglutaryl-CoA reductase in the protozoan *Trypanosoma cruzi*

Javier PEÑA-DÍAZ, Andrea MONTALVETTI, Ana CAMACHO, Claribel GALLEGO, Luis M. RUIZ-PEREZ and Dolores GONZALEZ-PACANOWSKA*

Instituto de Parasitología y Biomedicina 'López-Neyra', Consejo Superior de Investigaciones Científicas, C/ Ventanilla 11, 18001 Granada, Spain

We report the isolation and characterization of a genomic clone containing the open reading frame sequence for 3-hydroxy-3-methylglutaryl-CoA (HMG-CoA) reductase from *Trypanosoma cruzi*, the causative agent of Chagas' disease. The protozoan gene encoded for a smaller polypeptide than the rest of the genes described from eukaryotic organisms and the deduced amino acid sequence could be aligned with the C-terminal half of animal and plant reductases exhibiting pronounced similarity to other eukaryotic counterparts. Further examination of the 5′ flanking region by cDNA analysis and establishment of the splice acceptor sites clearly indicated that the corresponding mRNA apparently lacks sequences encoding a membrane N-terminal domain. The reductase gene is a single copy and is located on a chromosome of 1.36 Mb as determined by contour-clamped homogeneous electric field electrophoresis. The overall cellular distribution of enzymic activity was investigated after differential centrifugation of *Trypanosoma* cell extracts. Reductase activity was primarily associated with the cellular soluble fraction because 95 % of the total cellular activity was recovered in the supernatant and was particularly sensitive to proteolytic inactivation. Furthermore the enzyme can be efficiently overexpressed in a highly active form by using the expression vector pET-11c. Thus *Trypanosoma cruzi* HMG-CoA reductase is unique in the sense that it totally lacks the membrane-spanning sequences present in all eukaryotic HMG-CoA reductases so far characterized.

INTRODUCTION

Evidence presented by several laboratories has demonstrated that inhibitors of ergosterol biosynthesis interfere severely with the growth of protozoan parasites of the Trypanosomatidae family such as *Trypanosoma cruzi* and various *Leishmania* species [1,2]. Ergosterol is the principal sterol of the parasitic trypanosomatid flagellates [3] and it differs from cholesterol, the predominant mammalian sterol, by the presence of a 24-methyl group and Δ^7 and Δ^{22} bonds. Ergosterol biosynthesis inhibitors are effective antiproliferative agents that have been used in the treatment of diseases produced by fungi and yeast [4,5]. The basis of their effect is that ergosterol and related sterols are essential for viability and membrane function. One of the most widely used inhibitors is ketoconazole, an orally active imidazole antimycotic agent that exerts its effect by blocking the cytochrome *P*-450-dependent demethylation of lanosterol. In *T. cruzi*, the causative agent of Chagas' disease, for which there is no effective treatment, ketoconazole has been shown to have a trypanocidal activity although concentrations required for a parasitological cure were higher than those considered to be safe for human use [6]. Other inhibitors of the sterol biosynthetic pathway used in combination with ketoconazole clearly potentiate its effects. Urbina et al. [7] have shown with studies *in vivo* using a murine model of Chagas' disease that a combined treatment with mevinolin, an extremely potent competitive inhibitor of 3-hydroxy-3-methylglutaryl-CoA (HMG-CoA) reductase, and azole drugs such as ketoconazole was able essentially to eliminate circulating parasites and produce complete protection against death. In summary, the combined administration of ergosterol biosynthesis inhibitors that act at different points of the sterol biosynthetic pathway seems to be a promising strategy for the development of an effective treatment of Chagas' disease.

Apart from their effect on *T. cruzi*, the growth of bloodstream and culture-adapted procyclic forms of *Trypanosoma brucei* is also arrested by various inhibitors of HMG-CoA reductase [8]. Likewise, lovastatin and simvastatin inhibit the intra-erythrocytic development of *Plasmodium falciparum* and *Babesia divergens* and could represent new trends in antiparasitic chemotherapy in these organisms [9].

HMG-CoA reductase is the first committed step in the pathway of isoprenoid biosynthesis and catalyses the synthesis of mevalonic acid from HMG-CoA. This key enzyme has a crucial role in the production of the large family of molecules produced by the mevalonate pathway. Little is known about the nature and regulation of HMG-CoA reductase in parasitic protozoa; so far no characterization has been performed of a protozoan gene encoding for this enzyme. Whereas in bacteria HMG-CoA reductase is soluble [10,11], in all eukaryotic cells characterized the enzyme presents a variable N-terminal membrane domain and the major subcellular location seems to be the endoplasmic reticulum [12].

Here we describe the characterization of a *T. cruz*i HMG-CoA reductase gene lacking a membrane-domain coding sequence. This report is the first information on a soluble enzyme in an eukaryotic organism and eventually will redefine and facilitate

Abbreviations: CHEF, contour-clamped homogeneous electric field; HMG, 3-hydroxy-3-methylglutarate; HMG-CoA, 3-hydroxy-3-methylglutaryl-CoA; IPTG, isopropyl β-D-thiogalactoside; RT–PCR, reverse transcriptase–PCR; *tchmgr*, *Trypanosoma cruzi* 3-hydroxy-3-methylglutaryl-CoA reductase gene.

* To whom correspondence should be addressed.

The nucleotide sequence results reported here will appear in DDBJ, EMBL and GenBank Nucleotide Sequence Databases under the accession number L78791.

studies on the organization and regulation of the isoprenoid biosynthetic pathway in parasitic protozoa.

EXPERIMENTAL

Materials

Restriction enzymes, T4 DNA ligase, *Taq* polymerase and the Klenow fragment of DNA polymerase from Boehringer Mannheim were used under conditions specified by the manufacturer. [α-^{32}P]ATP was from ICN Pharmaceuticals (Irvine, CA, U.S.A.), D,L-[3-^{14}C]3-hydroxy-3-methyl-CoA and Hybond-N filters were from Amersham Iberica, and *R*,*S*-[5-^{3}H(N)]mevalonolactone was from NEN–Dupont. Aprotinin, trypsin inhibitor, sodium phosphate, dithiothreitol and BSA were from Sigma Chemical Co. PMSF and leupeptin were from Boehringer Mannheim, and Aquasol-2 was from NEN–Dupont. Oligonucleotides ATG-HMGR (5′-GGAATTCCATATGTTTCGTAGGGCAATTC-T-3′) and TGA-HMGR (5′-CGCGGATCCTCACTTCTTCT-TGCGATTCAG-3′) were synthesized at the Analytical Services of the Instituto de Parasitología y Biomedicina 'López-Neyra', Granada.

General procedures

Epimastigotes of *T. cruzi* were grown in filter-sterilized LIT medium with 10 % (v/v) heat-inactivated fetal calf serum (Gibco), in tissue culture flasks at 28 °C. Axenic cultured amastigote-like forms were obtained as described by Ley et al. [13]. Total *T. cruzi* genomic DNA was isolated from *T. cruzi* Y strain by phenol extraction [14]. Standard molecular biology techniques were performed as described [15].

Isolation of the *T. cruzi* HMG-CoA reductase gene (*tchmgr*) and DNA sequencing

The hybridization probe for screening for *tchmgr* was obtained by the PCR technique. Oligonucleotides HMG1 [5′-CTCGGAATTCATGGG(ACGT)ATGAA(CT)ATG-3′] and HMG2 [5′-CTCGAAGCTT(ACGT)CC(ACG)CG(ACGT)CC-(CT)TC(AGT)AT-3′], derived from highly conserved sequences of the catalytic domain, were synthesized in a Millipore ConSep LC500 DNA synthesizer and used as PCR primers. The reaction mixture (50 μl) contained 25 pmol of each of the two oligonucleotide primer mixtures HMG1 and HMG2, 500 ng of *T. cruzi* genomic DNA, dNTPs each at 400 μM, 50 mM KCl, 10 mM Tris/HCl, pH 8, and 1.5 mM $MgCl_2$. Amplification was initiated with 1.5 units of *Taq* polymerase. PCR parameters were 35 thermal cycles consisting of 1 min of denaturation at 94 °C followed by a 1.5 min annealing period at 45 °C and a 2 min extension period at 72 °C. Approximately 100000 plaques of a *T. cruzi* genomic library constructed in λEMBL3 were replica-plated on nitrocellulose and screened as described [15]. Sequencing was performed with the Sanger dideoxy termination method in a Applied Biosystem 373 DNA Sequencer. Appropriate primers were synthesized by using as a model both DNA strands from the coding region.

Construction and screening of a cDNA library

An expression cDNA library of *T. cruzi* Y strain was constructed with the ZAP Express® cDNA Synthesis Kit (Stratagene) by using 5 μg of poly(A)$^+$ mRNA obtained with the Quick Prep Micro mRNA Purification Kit (Pharmacia). The entire coding sequence of the *tchmgr* gene was amplified by PCR, using as primers oligonucleotides complementary to bp -15 to -1 and $+1435$ to $+1454$, and used as hybridization probe after labelling by the random primer method. Hybridization and washings were conducted at 42 °C. Approximately 100000 plaques were replica-plated on nitrocellulose and screened in accordance with standard protocols [15]. Phagemids were rescued from the library by co-infection of *Escherichia coli* XLIB with 2×10^5 plaque-forming units of λ phage and 10^6 plaque-forming units of ExAssist helper phage in 25 ml of Luria broth. The supernatant obtained after incubation and clarification of culture by centrifugation had a titre of 2.5×10^3 kanamycin-resistant colony-forming units/ml. The isolation of plasmid DNA was performed by the Wizard® Maxipreps DNA Purification System (Promega).

Contour-clamped homogeneous electric field (CHEF) electrophoresis

To locate the chromosome(s) containing the HMG-CoA reductase gene, CHEF electrophoresis was performed. Blocks of *T. cruzi* in low-melting-point agarose were prepared as described [16]. Chromosomes were separated on a 1 % (w/v) agarose gel with a CHEF system (Pharmacia). The following parameters were used: frequencies of 350 s for 24 h, frequencies of 500 s for 24 h, frequencies of 750 s for 24 h and frequencies of 1000 s for 24 h at 84 V and 13 °C. Molecular masses of the chromosomal DNA bands were determined by comparison with DNA standards from *Saccharomyces cerevisiae* strain S13. The resulting gel was transferred to a Hybond-N (Amersham) nylon filter and subjected to Southern blot analysis with the PCR amplified *tchmgr* gene as probe.

Construction of expression system

For expression in *E. coli*, the entire coding sequence was amplified by the PCR technique. The reaction mixture (50 μl) contained 25 pmol of each of the two oligonucleotide primers ATG-HMGR and TGA-HMGR, 100 ng of pHMGR4.3 DNA, dNTPs each at 400 μM, 60 mM KCl, 25 mM Tris/HCl, pH 8, 10 mM $MgCl_2$ and 0.1 % BSA. Amplification was initiated with 1.5 units of *Taq* polymerase. PCR parameters were 35 thermal cycles consisting of 60 s of denaturation at 94 °C followed by a 90 s annealing period at 65 °C and a 2 min extension period at 72 °C. Oligonucleotide primers for amplification of the HMG-CoA reductase coding sequence were designed so that *Nde*I and *Bam*HI restriction sites were introduced at the 5′ and 3′ ends for convenient cloning in the expression vector pET-11c to give pETHMGR, which was originally cloned and propagated in XL1B. Double-stranded DNA sequencing was performed to confirm the correct sequence after amplification. Subsequently pETHMGR was used to transform the *E. coli* expression host BL21(DE3). Bacterial clones were grown in Luria broth containing 50 μg/ml ampicillin. When induction was performed, bacterial cells transformed with pETHMGR were first grown at 37 °C to an A_{600} of 0.6 and then 1 mM isopropyl β-D-thiogalactoside (IPTG) was added; cultures were then grown for 2.5 h at 37 °C; cells were collected by centrifugation and, when not used immediately, frozen at -80 °C.

Northern blot and reverse transcriptase (RT)–PCR analysis

Poly(A)$^+$ mRNA was subjected to electrophoresis on 1 % (w/v) agarose gels containing 1 × Mops buffer [20 mM Mops/0.08 M sodium acetate (pH 7.0)/1 mM EDTA] and 6.29 % (v/v) formaldehyde after the samples had been boiled for 10 min in 50 % (v/v) formamide, 1 × Mops buffer and 5.9 % (v/v) formaldehyde. A 0.24–9.5 kb RNA ladder (Gibco) was used as a standard. The

gel was transferred to a Hybond-N filter and hybridized with the probe containing the entire coding sequence of the *tchmgr* gene amplified by PCR.

For mapping the splice acceptor site, cDNA was synthesized, using as primer an oligonucleotide complementary to positions +442 to +459 of the *tchmgr* gene (HMG-3; see Figure 2). The resulting cDNA was used as template in a first PCR, using as primers HMG-3 and a 23-mer complementary to the 3′ end of the splice leader (23-SL) sequence of *T. cruzi* [17]. The reaction product was diluted and used as template in a second PCR reaction, using as primers 23-SL and an oligonucleotide complementary to nucleotide positions +228 to +245 (HMG-4; see Figure 2). The reaction products were separated by gel electrophoresis and hybridized with the *tchmgr* gene.

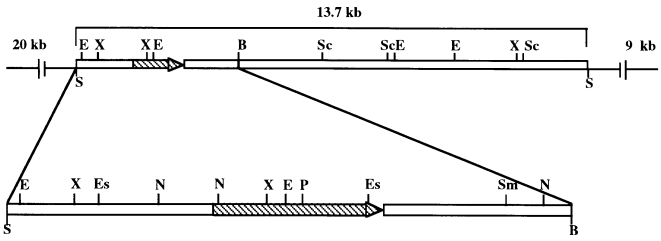

Figure 1 Restriction map of genomic DNA encompassing the *tchmgr* gene

The hatched area represents the coding region. Abbreviations: E, *Eco*RI; S, *Sal*I; X, *Xho*I; B, *Bam*HI; Sc, *Sac*I; Sm, *Sma*I; P, *Pst*I; N, *Nco*I; Es, *Esp*I.

Measurement of HMG-CoA reductase activity

T. cruzi pellets were suspended in buffer A (0.25 M sucrose/10 mM Hepes, pH 7.4/50 mM NaCl/20 mM EDTA/2 mM EGTA/5 mM dithiothreitol) containing 50 μg/ml aprotinin, 20 μg/ml leupeptin, 10 mM 1,10-phenanthroline, 1 mM benzamidine, 50 μg/ml trypsin inhibitor and 50 μM PMSF as protease inhibitors. The activity of HMG-CoA reductase was measured by the method of Shapiro et al. [18] and expressed as pmol of [^{14}C]HMG-CoA converted to [^{14}C]mevalonate/min per mg of protein. The incubation mixture consisted of 75 mM EDTA, 5 mM dithiothreitol, 90 mM glucose 6-phosphate, 9 mM NADP, 1.2 mM [^{14}C]HMG-CoA, 150 m-units of glucose-6-phosphate dehydrogenase and 25–50 μg of *T. cruzi* protein in a final volume of 75 μl. Samples were incubated for 15 min at 37 °C and reactions were stopped by the addition of 25 μl of 5 M HCl. [^{3}H]Mevalonolactone was added to the samples as an internal standard. Spectrophotometric determinations of reductase activity were performed as described by Frimpong et al. [19]. Protein was determined by the method of Bradford [20], with BSA as a standard.

RESULTS AND DISCUSSION

Genomic DNA cloning

The PCR probe was obtained by amplification of a fragment of the *tchmgr* gene, using as primers degenerate nucleotides complementary to highly conserved regions contained within the soluble catalytic domain and genomic *T. cruzi* DNA as template. Restriction sites (*Eco*RI and *Hin*dIII) were added to the 5′ end of each primer mixture to facilitate cloning of the PCR products. Several products were obtained after amplification of *T. cruzi* DNA, although a PCR product of the expected size (167 bp) was identified. The positive fragment was cloned in pUC18 and the correct identity of the amplified band was confirmed by sequencing. A genomic DNA library constructed in λEMBL3 was screened with the specific PCR probe. Two positive clones were obtained in the first screening of approx. 100000 plaques. After the third screening one clone was selected for restriction mapping and further characterization. This clone contained a 13.7 kb *Sal*I–*Sal*I insert that possessed the complete coding region of the HMG-CoA reductase gene. A restriction map of the genomic DNA encompassing the *tchmgr* gene is shown in Figure 1. A *Bam*HI–*Sal*I restriction fragment was identified that hybridized strongly with the PCR probe. This 4.3 kb segment was inserted in pBSKS$^-$ to give pHMGR4.3 and sequenced on both strands by using universal and synthetic primers.

The complete coding sequence, together with 323 and 332 bases of the 5′ and 3′ flanking regions respectively, is shown in Figure 2. Prediction of the initiation codon was based on the comparison of the *T. cruzi* sequence with prokaryotic HMG-CoA reductase sequences and the identification of potential non-coding regions by similarity analysis of 5′ flanking regions of other protozoan genes and codon usage studies. The selected open reading frame presented a codon usage that strongly adjusts to the codon frequency described for other *T. cruzi* genes. In addition, there were multiple TA repeats and a poly(T) tract characteristic of non-coding regions of genes from *T. cruzi*, *T. brucei* and *P. falciparum*. Finally, one terminator codon in the same reading frame was found 114 bp 5′ to the initiator methionine codon. No intervening sequences were identified. Translation of the open reading frame of 1305 bp yielded a polypeptide of 435 residues with an estimated molecular mass of 46100 Da.

The predicted amino acid sequence from the *tchmgr* gene was aligned by using Pileup (GCG Program Manual for the Wisconsin Package, version 8.0) with the sequences of the yeast, human, *Pseudomonas mevalonii* and *Haloferax volcanii* genes to optimize their sequence similarity, revealing a number of unique features of the *T. cruzi* protein (Figure 3). First, *tchmgr* encodes for a smaller polypeptide than the other genes described from eukaryotic organisms. The amino acid sequence aligns with the C-terminal half of animal and plant HMG-CoA reductases and exhibits pronounced similarity to other eukaryotic counterparts. Secondly, alignment analysis and hydrophobicity plots indicated that the enzyme totally lacks the membrane N-terminal domain characteristic of all eukaryotic HMG-CoA reductases characterized so far. The N-terminus of the reductase protein aligned with the N-terminal region of the *P. mevalonii* and Archaebacteria enzymes, prokaryotic representatives that also lack a membrane spanning domain. All of the conserved residues involved in catalysis or binding identified in other HMG-CoA reductases are present in the *T. cruzi* sequence. Of interest was the existence of an SKL-like sequence (MRL) in position 428 (seven residues from the stop codon) characteristic of the C-terminus of protozoan proteins that undergo glycosomal import [21]. This signal sequence, known as PTS-1, is present in the C-terminus of several peroxisomal proteins and has been shown to target proteins to the peroxisomes of mammals, plants, insects, fungi and yeast [22]. Whether it has any function in the intracellular targeting of *T. cruzi* HMG-CoA reductase might be further determined by transfection experiments of mutants designed for this purpose.

Northern blot analysis and characterization of the 5′ termini of HMG-CoA reductase transcripts

To establish the location of the translation initiation site and the absence of sequences encoding a membrane domain, a *T. cruzi* cDNA library constructed in the bacteriophage vector ZAP

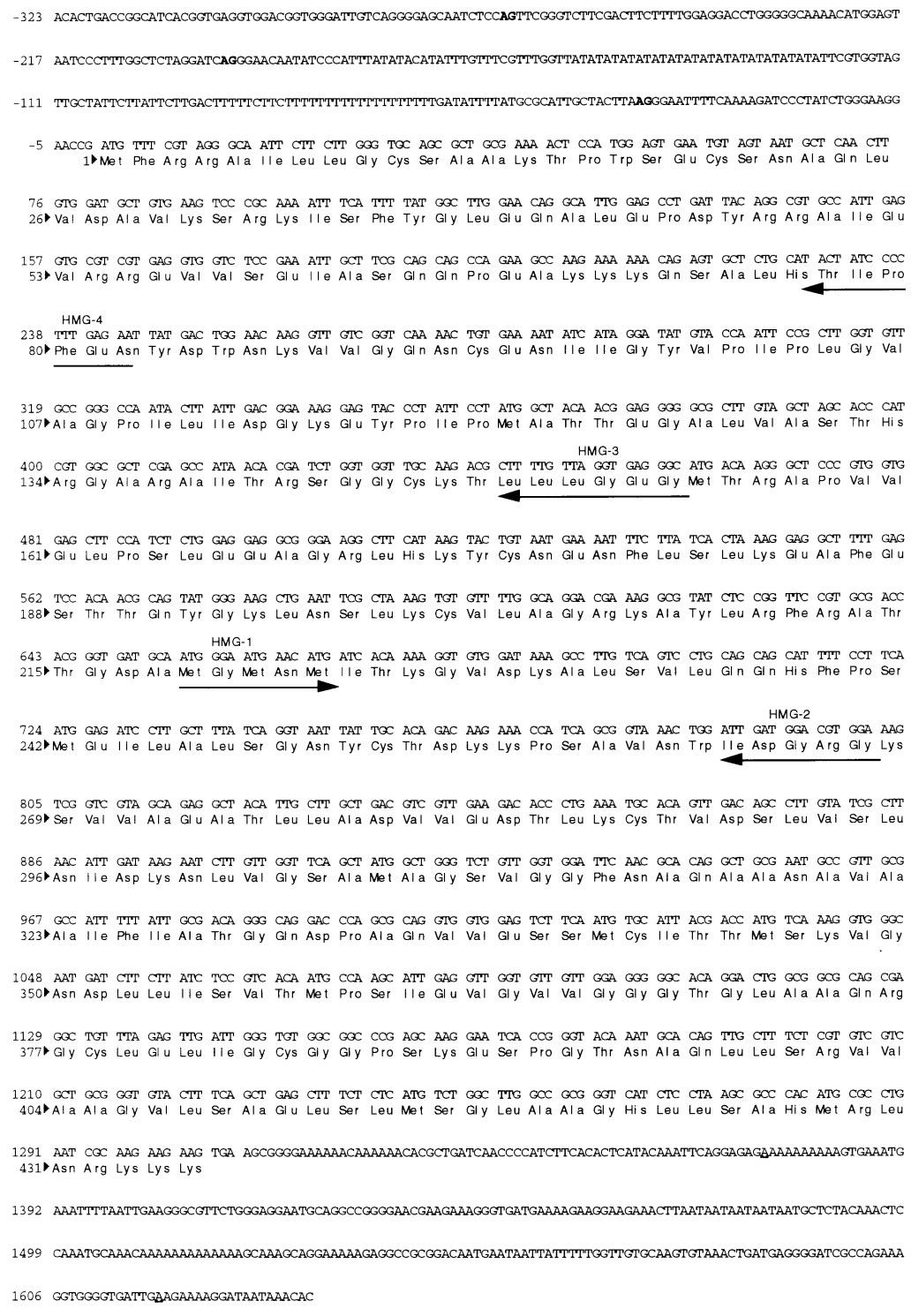

Figure 2 Genomic sequence of the *tchmgr* gene and portions of its flanking regions

The splice acceptor sites are indicated in bold letters. Polyadenylation sites are underlined. Arrows refer to sequences complementary to the primers used for amplification of the PCR probe used for screening the genomic library (HMG-1, HMG-2) and to primers used in the RT–PCR analysis for mapping of the splice acceptor site (HMG-3, HMG-4).

Express (Stratagene) was screened with the *tchmgr* gene. Trypanosomatids lack intervening sequences and most genes are transcribed as polycistronic transcription units, which are subsequently converted into monocistronic mRNAs by trans-splicing, which involves cleavage at the 5′ boundary of the protein coding region and the addition of a capped 39-nucleotide mini-exon (or splice leader) sequence to the newly generated 5′ end. Two positive clones were identified and used for sequencing the 5′ region, which revealed in both cases at position −38 a portion of the sequence characteristic of the 39-nucleotide spliced

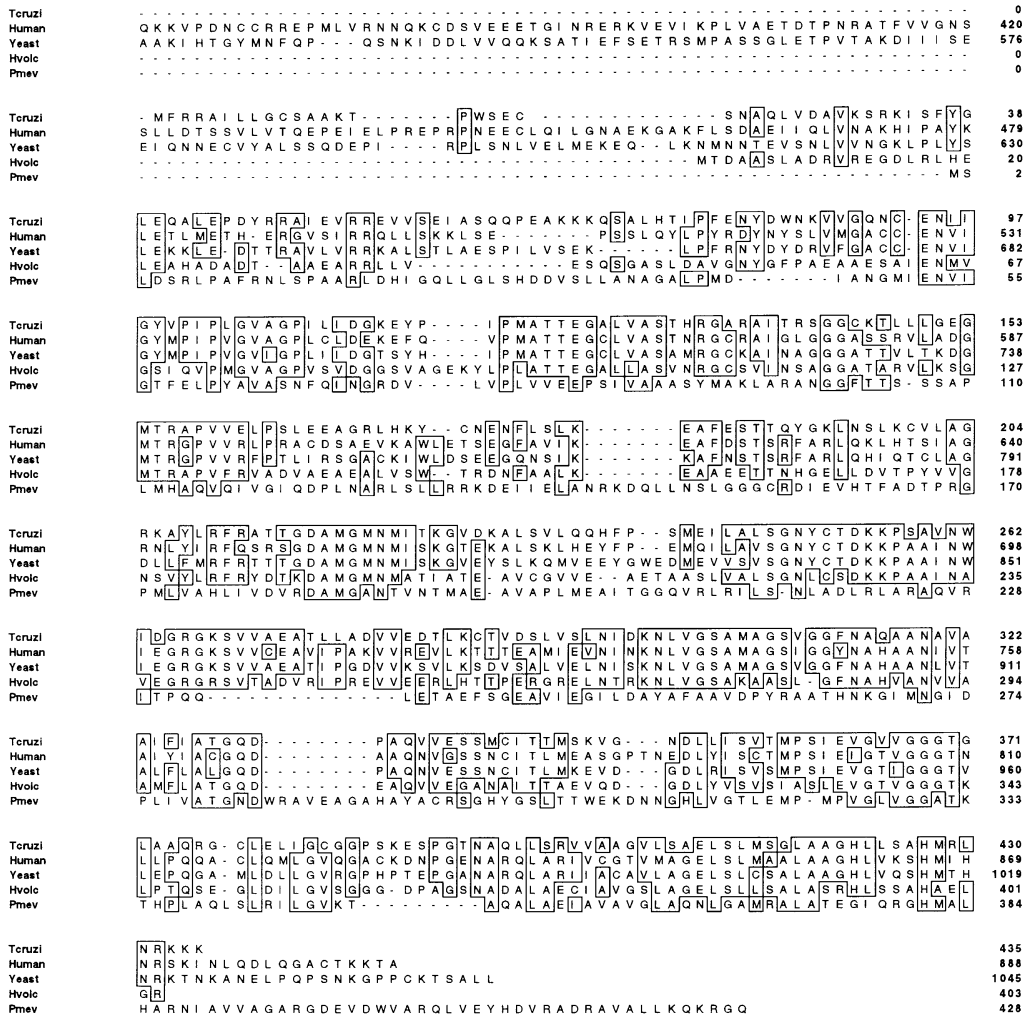

Figure 3 Comparison of the deduced amino acid sequence of *T. cruzi* HMG-CoA reductase with other reductases

The deduced amino acid sequence of *T. cruzi* HMG-CoA reductase is compared with the sequences of the human (residues 361–888), yeast (yeast HMG-CoA reductase isoenzyme 2, residues 520–1045), *Haloferax volcanii* (Hvolc) and *Pseudomonas mevalonii* (Pmev) reductases. Solid boxes indicate regions of amino acid sequence identity.

leader of *T. cruzi* [17]. The situation of the spliced leader corresponds in the genomic sequence with the dinucleotide AG distinguishing the splice acceptor site (Figure 2) and is downstream of a pyrimidine tract that conforms to the consensus motif for trans-splicing. The identification of the site of addition of the spliced leader sequence further supports the position of the ATG initiation codon and the supposition that a membrane-coding sequence is absent. The 3′ flanking region of the cDNA clones was also fully sequenced to determine the exact position of the poly(A) tail in these clones. Two different polyadenylation sites were identified in the two different cDNA clones at positions +1374 and +1619 and are indicated in Figure 2.

A Northern blot of poly(A)$^+$ RNA extracted from both epimastigote and amastigote forms of the parasite was performed with *tchmgr* as probe. The analysis indicated a transcript size of 2.2 kb for both forms of the parasite. A prolonged exposure of the autoradiogram did not reveal any additional bands and therefore the size of the mRNA determined by cDNA analysis might correspond to minor forms not readily observable in a Northern blot. The existence of additional splice acceptor sites to that already determined was considered as a potential explanation for the larger transcript. To analyse this possibility, RT–PCR was performed on epimastigote poly(A)$^+$ RNA with primers complementary to the *T. cruzi* HMG-CoA reductase sequence and to the splice leader sequence. The final PCR product obtained as indicated in the Experimental section was separated by gel electrophoresis: three bands were obtained when hybridized with the *tchmgr* probe (results not shown). The sizes of the different bands were calculated and the values obtained allowed for the establishment of two additional splice sites. Thus, apart from the band corresponding to the site in position −38, the two larger bands indicated two more splice sites located at positions −196 and −267 (Figure 2). However, the position of the two additional splice acceptor sites did not explain the size of the transcript observed in the Northern blot. The existence of another polyadenylation site not identified in this study could be an explanation. In summary, *tchmgr* pre-mRNA undergoes alternative splicing to give rise to transcripts that differ in the lengths of their 5′ leader sequences, but extensive sequences coding for a membrane domain were not evidenced. It will be of interest to determine the consequences, if any, of alternative splicing on the expression of HMG-CoA reductase.

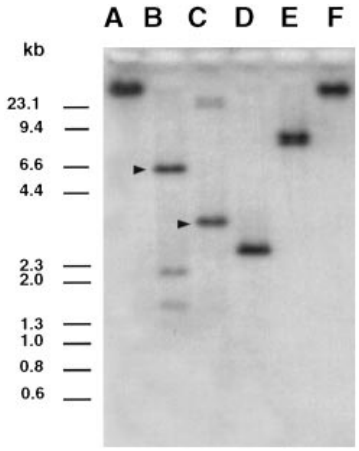

Figure 4 Southern blot analysis of *T. cruzi* genomic DNA

Total genomic DNA was digested with *Eco*RI (lane B), *Pst*I (lane C), *Nco*I (lane D) *Bam*HI (lane E) and *Sal*I (lane F); lane A, undigested DNA. The DNA fragments were separated in 1% (w/v) agarose, transferred to nitrocellulose and hybridized with the HMG-CoA reductase coding sequence. Arrowheads show the bands that did not hybridize with a probe spanning the first 475 bp of the HMG-CoA reductase coding sequence.

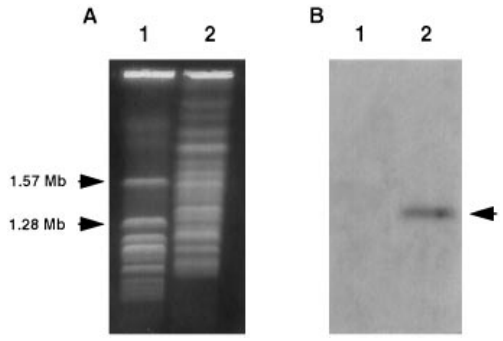

Figure 5 CHEF electrophoresis of chromosomes from *T. cruzi*

(**A**) Ethidium bromide-stained gel. Lane 1, *S. cerevisiae* as molecular mass marker chromosomes; lane 2, *T. cruzi* chromosomes. (**B**) Autoradiograph of a nylon transfer of the gel shown in (**A**) probed with the ^{32}P-labelled *tchmgr* probe.

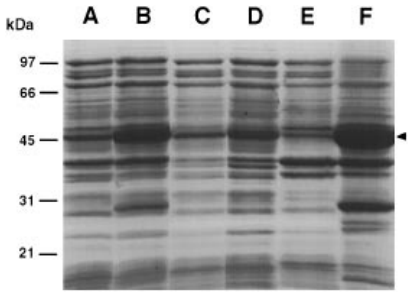

Figure 6 SDS/PAGE analysis of *T. cruzi* HMG-CoA reductase expression in *E. coli*

Lane A, crude extract from pET-11c-transformed cells; lane B, crude extract from pETHMGR-transformed cells; lane C, soluble fraction from pET-11c-transformed cells; lane D, soluble fraction from pETHMGR-transformed cells; lane E, insoluble fraction from pET-11c-transformed cells; lane F, insoluble fraction from pETHMGR-transformed cells. The gel was stained with Coomassie Blue; the positions of molecular mass standards are indicated at the left. The arrowhead indicates the position to which recombinant HMG-CoA reductase migrated.

Chromosomal localization and genomic organization of the *tchmgr* gene

Genomic DNA from a clone of *T. cruzi* Y strain was digested with different endonucleases, blotted and probed with a fragment that encompasses the entire coding region of the HMG-CoA reductase gene (Figure 4). Lanes B and C correspond to digestions with endonucleases *Eco*RI and *Pst*I that present unique restriction sites within the coding region. Lanes D, E and F in Figure 4 correspond to digestions with *Nco*I, *Bam*HI and *Sal*I (sites outside the coding region). In digestions with *Eco*RI and *Pst*I there was hybridization to an extra band that would not have been predicted considering the restriction map of the λEMBL3 clone isolated in the screening process. The extra band was approximately 500 bp smaller than would have been expected from the restriction map obtained for the library genomic clone and presented an equal intensity to one of the other two bands. Likewise, digestions with *Bam*HI and *Sal*I yielded two bands, whereas digestion with *Pst*I (a site that is approx. 700 bp from the ATG start codon) gives one only band. Genomic digests hybridized with a probe spanning the first 475 bp of the HMG-CoA reductase coding sequence clearly showed that the size polymorphism was located in the 5′ region of the reductase gene, whereas the 3′ region was highly similar (Figure 4). We conclude that *tchmgr* exists as single copy but that size polymorphism exists in the 5′-flanking region between alleles so that a 500 bp region is absent from one of them. The deletion is contained within an *Eco*RI–*Eco*RI fragment that also contains the N-terminus of *T. cruzi* reductase. Complete sequencing of the 4.3 kb fragment from the λEMBL3 clone revealed the existence of additional unidentified ORFs 5′ and 3′ to the reductase gene, further supporting the supposition that it is not tandemly repeated.

In several protozoa the chromatin is poorly condensed during mitosis and distinct chromosomes cannot be detected. However, the chromosomes of *T. cruzi* range in size between 450 kb (or even smaller) and 2.5 Mb [23] and can be resolved by CHEF electrophoresis. The intensities of the different chromosomal bands vary, reflecting the presence of multiple chromosomes in some of the bands, yet complete resolution of all chromosomal bands is not possible even if conditions are optimized for different size ranges. The present electrophoresis was performed under conditions that favoured the separation of the larger chromosomal bands, and the *tchmgr* gene labelled by random priming was used to hybridize the filter replicate of chromosomes. As shown in Figure 5, under the CHEF conditions used in this study HMG-CoA reductase sequences were located on a single chromosome of 1.36 Mb.

Expression of the *tchmgr* gene in *E. coli*

Further work on *T. cruzi* HMG-CoA reductase depends on the ability to generate sufficient quantities of the enzyme to perform a detailed structural and kinetic characterization. To enhance the level of expression, the entire coding region identified was amplified by PCR, placed in the expression vector pET-11c (Stratagene) to give pETHMGR and used to transform BL21(DE3) cells. Lysates of cells induced for 2.5 h with IPTG displayed a 46 kDa band not present in cells transformed with the vector alone (Figure 6). Densitometric scanning of stained

Table 1 Distribution of HMG-CoA reductase activity in *T. cruzi* extracts

S_9 refers to the whole supernatant obtained after sonication and centrifugation at 9000 ***g***; S_{105} and P_{105} refer to the supernatant and pellet respectively obtained after centrifugation of S_9 at 105000 ***g*** for 60 min. Values are the averages of four determinations. Standard deviations did not exceed 10% of the average value.

	HMG-CoA reductase activity					
	Specific activity (pmol/min per mg)			Total activity (pmol/min)		
	S_9	S_{105}	P_{105}	S_9	S_{105}	P_{105}
Without protease inhibitors	161	251	589	678	533	495
With protease inhibitors	6212	6865	999	34478	25821	1648

gels showed that the level of *T. cruzi* HMG-CoA reductase was approximately 3–5% of soluble protein in *E. coli* containing the expression construct. The enzyme was highly active, which permitted determinations with a spectrophotometric assay. The specific activity of soluble extracts of IPTG-induced *E. coli* recombinants was approx. 1600 nmol/min per mg, 257-fold that obtained with crude extracts from *T. cruzi* (Table 1).

HMG-CoA reductase activity in *T. cruzi* extracts

T. cruzi epimastigote cells were grown to exponential phase (60×10^6 cells/ml), collected by centrifugation, washed with PBS and resuspended immediately in buffer A with or without protease inhibitors. Cells were ruptured by mild sonication with a microprobe four times for 30 s on the 50% duty pulse setting. The extract was clarified by centrifugation (9000 ***g***, 10 min, 4 °C) and further centrifuged at 105000 ***g*** for 60 min at 4 °C in a Beckman Optima TLX Ultracentrifuge. The resulting pellet was resuspended in buffer A with or without protease inhibitors, and both the pellet and the 105000 ***g*** supernatant were used as enzyme source for determination of reductase activity. As shown in Table 1, *T. cruzi* reductase activity was severely decreased in the absence of protease inhibitors. This effect was more pronounced in the 105000 ***g*** supernatant, where specific activity was 38-fold higher when protease inhibitors were included in the sonication buffer. In contrast with other eukaryotic cells, the specific activity in the supernatant was 7-fold that obtained in the pellet or 'membrane' fraction. In addition, when the total activity recovered in each fraction was calculated, 95% of the total enzyme activity was located in the supernatant. The specific activity of the enzyme in *T. cruzi* epimastigotes is extremely high, approximately one order of magnitude higher than in hepatocytes (reported as 350–400 pmol/min per mg), which exhibit notable isoprenoid biosynthetic rates. The biological significance of such an elevated enzymic activity is unclear at present but suggests the possibility that isoprenoid biosynthesis occurs at a high rate and is required for adequate growth. Nevertheless, previous reports have shown that sterol synthesis is not always proportional to reductase levels and was not increased in compactin-resistant cells that presented 400-fold more enzyme molecules [24]. The HMG-CoA content and overall biosynthetic rates should be determined to clarify the significance of such a high activity in relation to isoprenoid synthesis capability.

In support of the present report indicating the absence of a membrane-spanning domain and the existence of a soluble form of reductase is a set of detailed evidence indicating that enzyme activity is associated with the glycosomal subcellular fraction and not with the endoplasmic reticulum or plasma membrane (J. L. Concepción, J. A. Urbina and D. Gonzalez-Pacanowska, unpublished work). Coppens et al. [8] have reported that in *T. brucei* HMG-CoA reductase activity is located within the endoplasmic reticulum and subject to regulation, presumably through the cytosolic concentration of products of the mevalonate pathway [8,25]. However, the present study performed in the presence of protease inhibitors suggests that although both belong to the *Trypanosoma* genus, in *T. cruzi* an HMG-CoA reductase protein exists in a soluble form.

The fact that a membrane domain is absent might have important implications in the regulatory or functional properties of enzymic activity. The different eukaryotic HMG-CoA reductases characterized present a highly similar catalytic domain fused to a variable N-terminal region that contains membrane-spanning sequences responsible for anchorage in the endoplasmic reticulum; nevertheless the catalytic domain can function in the absence of the membrane domain. Studies on the mammalian enzymes have shown that the N-terminal membrane anchor is both necessary and sufficient for sterol- and non-sterol-accelerated degradation of the enzyme [26–28]. In the archaebacterium *Halobacterium halobium*, which presents a soluble HMG-CoA reductase, maximum activity is achieved in 3.5 M KCl and regulation in response to mevalonate availability occurs at the level of HMG-CoA concentration and not reductase activity [29]. In view of these multiple regulatory strategies, the identification of the components of the regulation of HMG-CoA reductase and isoprenoid synthesis in *T. cruzi* and studies on whether enzyme activity is responsive to mevalonate and sterols will further determine the consequences of the absence of a membrane domain on reductase control in these organisms. The characterization of the *T. cruzi* HMG-CoA reductase gene constitutes, to our knowledge, the first description of a eukaryotic reductase devoid of a membrane-spanning region and will prove to be useful as a model for studies in general on the kinetics and structure of eukaryotic reductases. Likewise, the development of an overexpression system will permit the availability of recombinant enzyme in high quantities for the performance of detailed mechanistic and structural studies; these might contribute towards a rational design of specifically targeted inhibitors against trypanosomal reductases that can take advantage of the unique localization of the enzyme in these organisms.

These studies were supported by grants from the UNDP/World Bank/WHO Special Program for Research and Training in Tropical Diseases (ID no.950526), the Dirección General de Investigación Científica y Técnica (PB93-0179) and the Plan Andaluz de Investigación (Cod. 3277). J. P. is a Predoctoral Fellow of the Spanish PFPI of the Ministerio de Educación y Ciencia, A.M. is a Predoctoral Fellow of the Instituto de Cooperación Iberoamericana, A.C. is a Predoctoral Fellow of the Plan Andaluz de Investigación and C.G. is a Predoctoral Fellow of the Fundación Ramón Areces.

REFERENCES

1 Urbina, J. A., Lazardi, K., Aguirre, T., Piras, M. M. and Piras, R. (1991) Antimicrob. Agents Chemother. **35**, 730–735
2 Berman, J. D., Goad, L. J., Beach, D. H. and Holz, Jr., G. G. (1986) Mol. Biochem. Parasitol. **20**, 85–92
3 Goad, L. J., Holz, Jr., G. G. and Beach, D. H. (1984) Mol. Biochem. Parasitol. **10**, 161–170
4 Ryder, N. S. (1988) Ann. N.Y. Acad. Sci. **544**, 208–220
5 Troke, P. F., Marriot, M. S., Richardson, K. and Tarbit, M. H. (1988) Ann. N.Y. Acad. Sci. **544**, 284–293
6 Urbina, J. A., Vivas, J., Visbal, G. and Contreras, L. M. (1995) Mol. Biochem. Parasitol. **73**, 199–210
7 Urbina, J. A., Lazardi, K., Marchan, E., Visbal, G., Aguirre, T., Piras, M. M., Piras, R., Maldonado, R. A., Payares, G. and DeSouza, W. (1993) Antimicrob. Agents Chemother. **37**, 580–591
8 Coppens, I., Bastin, P., Levade, T. and Courtoy, P. J. (1995) Mol. Biochem. Parasitol. **69**, 29–40

9 Grellier, P., Valentin, A., Millerioux, V., Schrevel, J. and Rigomier, D. (1994) Antimicrob. Agents Chemother. **38**, 1144–1148
10 Jordan Starck, T. C. and Rodwell, V. W. (1989) J. Biol. Chem. **264**, 17913–17918
11 Lam, W. L. and Doolittle, W. F. (1992) J. Biol. Chem. **267**, 5829–5834
12 Olender, J. L. and Simoni, R. D. (1992) J. Biol. Chem. **267**, 4223–4235
13 Ley, V., Andrews, N., Robbins, E. S. and Nussenzweig, V. (1988) J. Exp. Med. **168**, 649–659
14 Coderre, J. C., Beverley, S. M., Schimke, R. T. and Santi, D. V. (1983) Proc. Natl. Acad. Sci. U.S.A. **80**, 2132–2136
15 Ausubel, F. M., Brent, R., Kingston, R. E., Moore, D. D., Seidman, J. G., Smith, J. A. and Struhl, K. (eds.) (1987) Current Protocols in Molecular Biology, John Wiley and Sons, New York
16 Garvey, E. P. and Santi, D. V. (1986) Science **233**, 535–540
17 McCarthy Burke, C., Taylor, Z. A. and Buck, G. A. (1989) Gene **82**, 177–189
18 Shapiro, D. J., Nordstrom, H. L., Mitschelen, J., Rodwell, V. W. and Schimke, R. T. (1974) Biochim. Biophys. Acta **370**, 369–377
19 Frimpong, K., Darnay, B. G. and Rodwell, V. W. (1993) Prot. Exp. Purif. **4**, 337–344
20 Bradford, M. M. (1976) Anal. Biochem. **72**, 248–254
21 Sommer, J. M. and Wang, C. C. (1994) Annu. Rev. Microbiol. **48**, 105–138
22 Gould, S. J., Keller, G. A., Hosken, N., Wilkinson, J. and Subramani, S. (1989) J. Cell Biol. **108**, 1657–1664
23 Henriksson, J., Aslund, L. and Pettersson, U. (1996) Parasitology Today **12**, 108–114
24 Mosley, S. T., Brown, M. S., Anderson, R. G. W. and Goldstein, J. L. (1983) J. Biol. Chem. **258**, 13875–13881
25 Coppens, I. and Courtoy, P. J. (1995) Mol. Biochem. Parasitol. **73**, 179–188
26 Gil, G., Faust, J. R., Chin, D. J., Goldstein, J. L. and Brown, M. S. (1985) Cell **41**, 249–258
27 Jingami, H., Brown, M. S., Goldstein, J. L., Anderson, R. G. W. and Luskey, K. L. (1987) J. Cell Biol. **104**, 1693–1704
28 Skalnik, D. G., Narita, H., Kent, C. and Simoni, R. D. (1988) J. Biol. Chem. **263**, 6836–6841
29 Cabrera, J. A., Bolds, J., Shields, P. E., Havel, C. M. and Watson, J. A. (1986) J. Biol. Chem. **261**, 3578–3583

Received 7 October 1996/24 January 1997; accepted 7 February 1997